Dyes and Pigments 139 (2017) 747–755

Contents lists available at ScienceDirect

Dyes and Pigments

journal homepage: www.elsevier.com/locate/dyepig

Substitution effect of super hydrophobic units: A new strategy to design deep blue fluorescent emitters

Ke Li [a], Ming Liu [a], Shuai Yang [b], Yantong Chen [a], Yaowu He [a], Imran Murtaza [c], Osamu Goto [a], Clifton Shen [a], Hong Meng [a,*], Gufeng He [b,**]

[a] School of Advanced Materials, Peking University Shenzhen Graduate School, Peking University, Shenzhen, 518055, China
[b] Center for Opto-electronic Materials and Devices, Dept of Electronic Engineering, Shanghai Jiao Tong University, National Engineering Lab for TFT-LCD Materials and Technologies, 800 DongChuan Rd, Shanghai 200240, China
[c] Key Laboratory of Flexible Electronics (KLOFE) & Institute of Advanced Materials (IAM), Jiangsu National Synergetic Innovation Center for Advanced Materials (SICAM), Nanjing Tech University (NanjingTech), 30 South Puzhu Road, Nanjing 211816, China

ARTICLE INFO

Article history:
Received 25 October 2016
Received in revised form
15 December 2016
Accepted 15 December 2016
Available online 18 December 2016

Keywords:
Deep blue
Intermolecular packing
Material chemistry
OLED
Photoluminescence
Super hydrophobic

ABSTRACT

Fluorescent deep-blue emitters consisting of arylamine chrysene have attracted immense commercial interest in organic light-emitting devices (OLEDs). Herein, we endeavor to design emitters with super hydrophobic groups, namely trifluoromethoxy ($-OCF_3$) or trifluoromethylsufanyl ($-SCF_3$) substituted on 6,12-diarylamine chrysene. Surprisingly, the new materials show highly efficient and substantial blue shift in fluorescence spectra with more pure color quality, higher thermostability and better moisture resistant properties. Astonishing electroluminescence performance is envisioned by promoting the molecular design based on experience and theoretical calculations along with the single crystal X-Ray analysis. The CIE coordinate values for 6, 12-diamine-*N,N,N′,N′-tetra*(*p*-trifluoromethoxyphenyl)chrysene (DATPC-OCF_3) and 6,12-diamine-*N,N,N′,N′-tetra*(*p*-trifluoromethylsulfanylphenyl)chrysene (DATPC-SCF_3) are (0.14, 0.09) and (0.15, 0.06), respectively, which exactly match with the National Television System Committee (NTSC) and High-Definition Television requirements for unprecedented deep-blue emission.

1. Introduction

Since Tang et al. first demonstrated a multilayer device structure to achieve high efficiency in 1987 [1], organic light-emitting diodes (OLEDs) have been the most promising technology for the third generation displays [2]. However, pure blue emitter with high luminous efficiency (4–5 cd/A) and suitable Commission Internationale de L'Eclairage (CIE) coordinates of (0.12–0.15, 0.06–0.10) are still challenging [3,4]. Therefore, it is highly desirable to obtain a stable and high-performance blue emitter to make OLEDs with three primary colors. Although thermally activated delayed fluorescence (TADF) and phosphorescent OLEDs have recently obtained higher efficiency, fluorescent emitters are more competitive because of the more credible device performance and easier fabrication [5]. At present, only conventional fluorescent emitters have managed to realize large scale industrial production. High efficiency roll-off at high luminance and shorter lifetime are inherent drawbacks of TADF and phosphorescent OLEDs [6]. Fluorescent deep-blue emitters, arylamine substituted chrysene [7], are so far reported to be the best blue dopant material in OLEDs [8,9]. However, blue fluorescence emitters have external quantum efficiency (EQE) almost below 3% [10], low color purity and unstable lifetime, which are urgent problems to solve in all blue OLEDs [11].

Our work focuses on the design and development of an emitting material, comprising the prominent class of chrysene, to achieve tuned deep-blue color emission. In particular, we endeavor to accomplish novel high efficient deep blue emitters with super moisture resistant characteristics. Although tuning deep blue emission of the chrysene chromophores has been demonstrated through various substituted groups, only a little research work has been conducted to address the stability of emitting materials. It is widely accepted that one of the degradation pathways of OLEDs is electrochemical oxidation and reduction processes [12], most likely due to the oxygen and water effects. Thus, designing moisture resistant molecules with intrinsic hydrophobic properties will be

* Corresponding author.
** Corresponding author.
E-mail addresses: menghong@pkusz.edu.cn (H. Meng), gufenghe@sjtu.edu.cn (G. He).

http://dx.doi.org/10.1016/j.dyepig.2016.12.034
0143-7208/

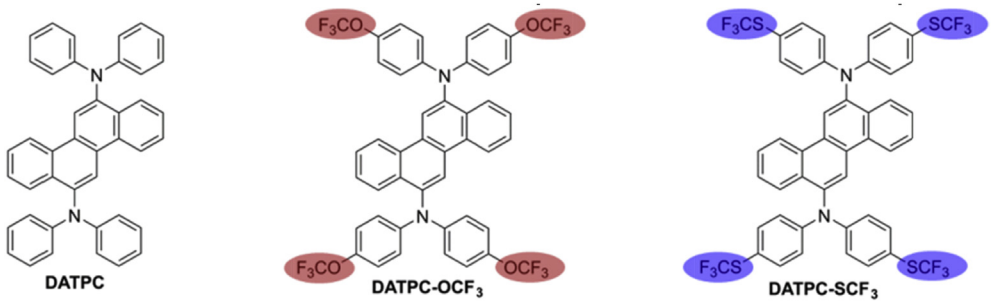

Scheme 1. Structures of DATPC, DATPC-OCF_3 and DATPC-SCF_3.

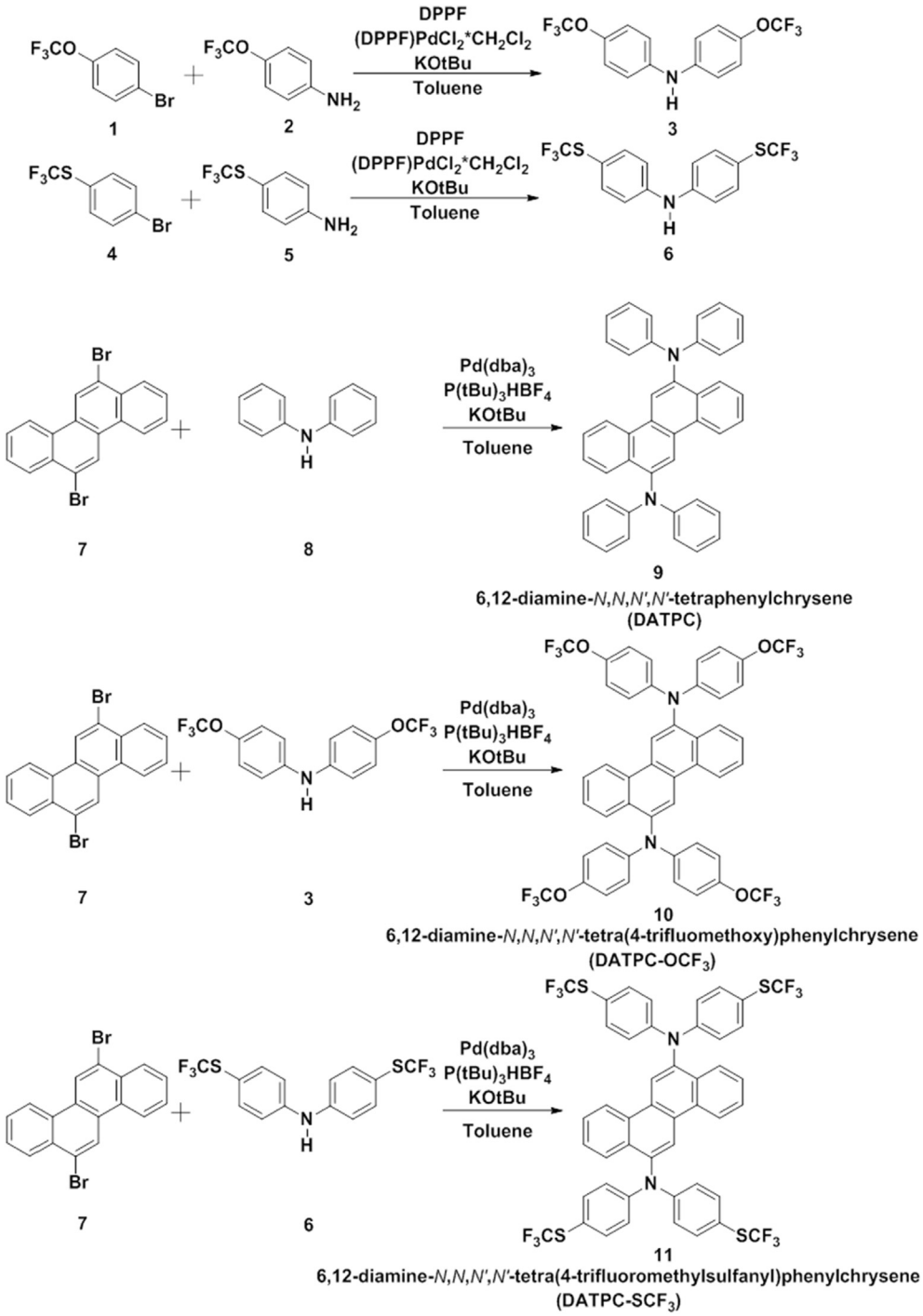

Scheme 2. Synthesis of 6,12-diphenylaminechrysene (DATPC) and its derivatives (DATPC-OCF_3 and DATPC-SCF_3).

beneficial for the stability of the OLEDs [13]. Considering the above issues, we strategically introduce super hydrophobic groups substitution to realize highly efficient deep blue luminance.

Trifluoromethoxy ($-OCF_3$) or trifluoromethylsufanyl ($-SCF_3$) groups, because of their super hydrophobic property have been remarkably used in agrochemicals, medical imaging and pharmaceuticals [14], owing to their high Hansch hydrophobicity parameter (π_R) of 1.04 and 1.44, respectively (compared to trifluoromethyl group with $\pi_R = 0.88$). Moreover, a relatively small overlap integral between the adjacent molecules is needed to realize fluorescent blue emission [15]. According to the equation, $E_g(eV) = \frac{1240}{\lambda(nm)}$, if we want to obtain a deep blue colored emitter, the bandgap should be increased. In other words, one useful strategy to get deep blue fluorescence is to introduce strong electron withdrawing groups to redistribute active electron density [16,17], or bulky substituents to obtain steric separation. The matter of rejoice is that $-OCF_3$ and $-SCF_3$ are also strong electron withdrawing groups [18]. Recently, the Jongwook Park group designed deep blue fluorescent emitters using the triphenylamine substituted chrysene achieving impressive high EQE [8]. However, 6,12-bis(triphenylamine)chrysene hardly makes any blue shift in luminescence spectra as compared to 6,12-diarylamine chrysene (DATPC). It may be due to the fact that arylamine groups do not efficiently distribute active electron density [19]. So we envisage that introducing $-OCF_3$ and $-SCF_3$ super hydrophobic and strong electron withdrawing groups can realize fluorescence emission sustaining blue shift and enhance the stability synergistically.

Herein, we demonstrate novel DATPC derivatives with *para*-substituted $-OCF_3$ and $-SCF_3$ groups in phenyl rings. Molecular structures of DATPC, 6,12-diamine-*N,N,N′,N′-tetra*(*p*-trifluoromethoxyphenyl)chrysene (DATPC-OCF_3) and 6,12-diamine-*N,N,N′,N′-tetra*(*p*-trifluoromethylsulfanylphenyl)chrysene (DATPC-SCF_3) are illustrated in Scheme 1 and their synthesis techniques are summarized in Scheme 2. The Density Functional Theory (DFT) calculation along with the single crystal X-ray analysis establish the correctness of design strategy. DATPC-OCF_3 and DATPC-SCF_3 show substantial blue shift in UV–vis absorption and fluorescence spectra.

The narrower full width at half maximum (FWHM) (49–50 nm) of absorption and fluorescence spectra as compared to DATPC (63 nm) imply higher color purity. Single layer undoped devices achieve maximum external quantum efficiency (EQE) of 3.05% and the CIE coordinate values of (0.14, 0.09) and (0.15, 0.06) for DATPC-OCF_3 and DATPC-SCF_3, respectively, which exactly meet the High-Definition Television ITU-R BT.709 requirement of CIE (0.15, 0.06) for deep-blue emission [11]. Based on the aforementioned facts, we report a simple fabrication process to obtain deep-blue and highly efficient novel emitters for OLEDs by incorporating super hydrophobic units of $-OCF_3$ or $-SCF_3$ substituted in 6,12-diarylamine chrysene.

2. Results and discussion

2.1. Theoretical calculations, the single crystal X-Ray analysis, physical and optical properties

DFT calculations (B3LYP/6-31G* as basis set) of the DATPC complexes were carried out to evaluate the effect of $-OCF_3$ and $-SCF_3$ substitution and the results are summarized in Fig. 1 and Table 1. As shown in Fig. 1, $-OCF_3$ and $-SCF_3$ substituent groups withdraw the HOMO electron to diphenylamine group, separating them from the LUMO electron concentrate on chrysene core. The theoretically predicted and experimental values of the bandgap (E_g) of DATPC are 3.4 eV and 2.81 eV, respectively. Actually, DATPC has sky blue-colored emission and according to $E_g(eV) = \frac{1240}{\lambda(nm)}$, if one

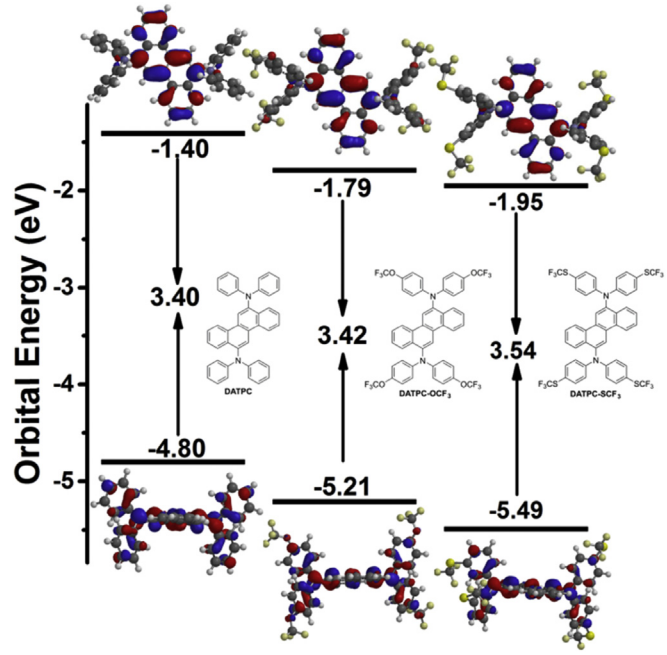

Fig. 1. Molecular structure; HOMO and LUMO electron density and orbital energy level at S_0 state calculated by the DFT B3LYP/6-31G* for DATPC, DATPC-OCF_3 and DATPC-SCF_3.

Table 1
Physical properties of DATPC, DATPC-OCF_3 and DATPC-SCF_3.

Compound	DFT calculation[a] (eV)			Experimental data (eV)		
	HOMO	LUMO	Bandgap	HOMO[b]	LUMO[c]	Bandgap
DATPC	−4.80	−1.40	3.4	−4.98	−2.17	2.81
DATPC-OCF_3	−5.21	−1.79	3.42	−5.28	−2.32	2.96
DATPC-SCF_3	−5.49	−1.95	3.54	−5.40	−2.38	3.02

[a] The S_0 states of the compounds calculated using B3LYP/6-31G* basis set.
[b] HOMO obtained from cyclic voltammetry.
[c] LUMO obtained from the HOMO and the optical bandgap.

wants to get a deep blue color emitter, the bandgap of new molecules should be wider than that of DATPC. Further comparison of the theoretical and experimental values of bandgaps of DATPC, DATPC-OCF_3 and DATPC-SCF_3 in Table 1, reveals that the values of their bandgaps follow the order: DATPC < DATPC-OCF_3<DATPC-SCF_3. It indicates fluorescence emission sustaining blue shift from DATPC to DATPC-SCF_3. Oxygen and sulfur atoms possess two additional pairs of non-bonding electrons [20], which lowers the HOMO more than the LUMO, it may be the net effect which causes the bandgap to increase. The enlarged bandgap is also attributed to slightly decreased intramolecular conjugation length [21,22]. Most importantly, $-OCF_3$ and $-SCF_3$ substitution is probably unique one to fine-tune and engineer the bandgap in order to achieve deep blue emission in highly efficient OLED materials.

The crystal structures of DATPC-OCF_3 and DATPC-SCF_3 are shown in Fig. 2 (a) and (b). Whereas for DATPC, it proved to be unfeasible to obtain the single crystal due to its instability. From single crystal X-ray structures, the corresponding dihedral angles between chrysene and phenyl groups of DATPC-OCF_3 and DATPC-SCF_3 are 87.61° and 89.43°, which are almost equal to right-angle. The DFT calculation shows that the torsion angles for DATPC, DATPC-OCF_3 and DATPC-SCF_3 are 77.77°, 85.04° and 87.54°, respectively, which are in good agreement and confirm the same order with the single crystal data. Thus, the bulky $-OCF_3$ and $-SCF_3$ substituents coincide with the former idea of steric separation to

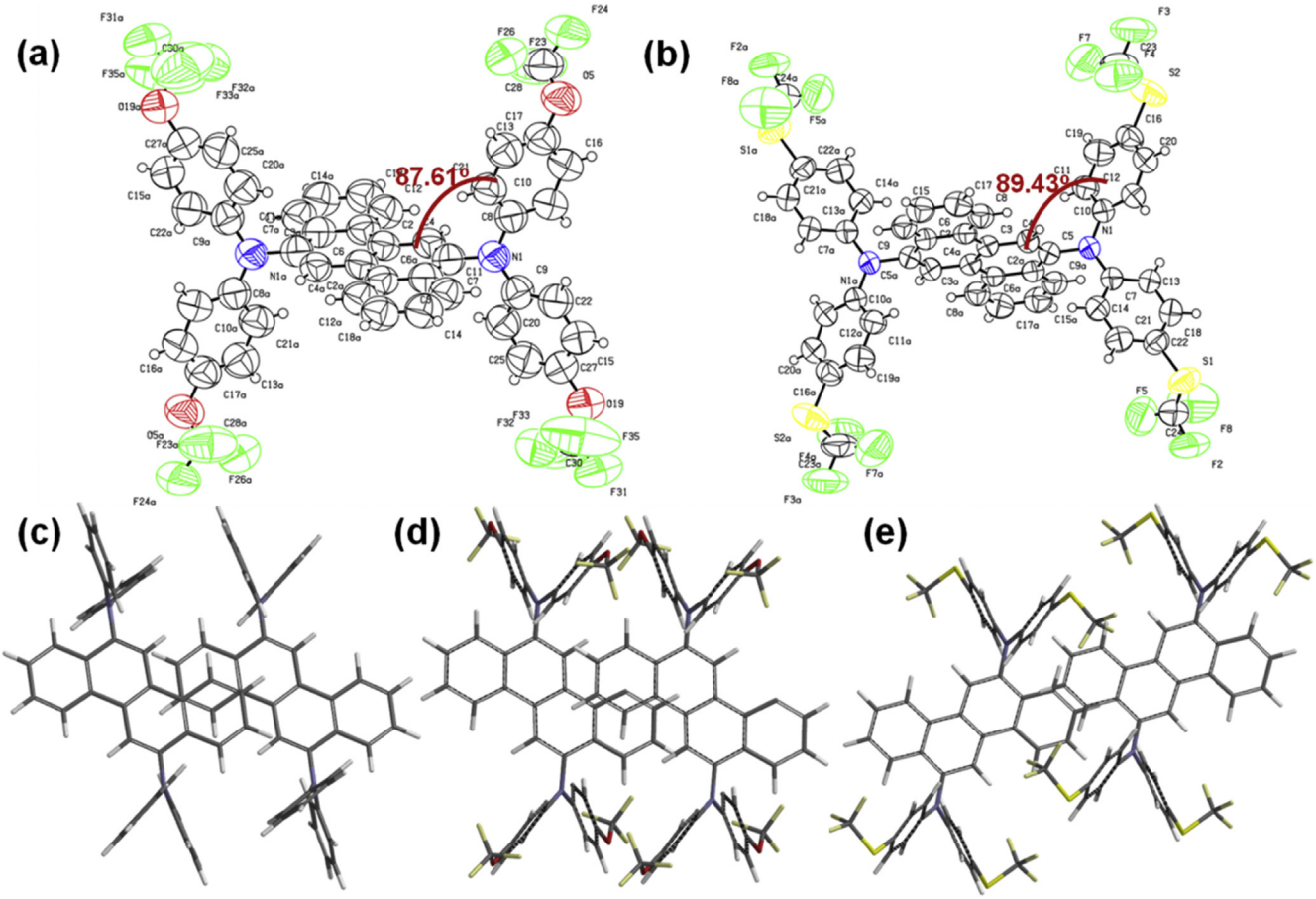

Fig. 2. The single X-ray crystal structure of (a) DATPC-OCF_3 and (b) DATPC-SCF_3. Molecular modeling method optimized dimer structures of (c) DATPC, (d) DATPC-OCF_3 and (e) DATPC-SCF_3. Highly-ordered molecular packing details of DATPC-OCF_3 and DATPC-SCF_3 in Fig. 3, it is obvious that DATPC, DATPC-OCF_3 and DATPC-SCF_3 all adopted J-type aggregation stacking columns [23]. The overlap percentage of two adjacent chrysene planes has gradually reduced from DATPC to DATPC-SCF_3.

realize high efficiency. Fig. 2 (c), (d) and (e) are the optimized dimer aggregation structures of DATPC, DATPC-OCF_3 and DATPC-SCF_3 by Spartan molecular modeling method. The aggregation overlap integrals of all the three dimers are very low and nearly no π-π interaction is observed. Combined with the single crystal X-ray.

Fig. 3 (a) and (b) are the highly-ordered molecular packing details of DATPC-OCF_3 and DATPC-SCF_3 respectively. This herringbone cross-lamination arrangement of chrysene core is significantly beneficial to reduce transportation distance of the excitons. In the case of DATPC-OCF_3, the shortest intermolecular distance is 3.47 Å (from hydrogen atom to fluorine atom). For DATPC-SCF_3, the shortest distance between two adjacent molecules is 2.55 Å (from hydrogen atom to fluorine atom). In fact, these shorter distances promote intermolecular exciton transfer. The intermolecular chrysene-chrysene distances obtained from single X-ray crystal data of DATPC-OCF_3 and DATPC-SCF_3 are 3.434 Å and 3.330 Å, respectively, where it is generally accepted that high-efficient intermolecular interaction often occurs within effective distance smaller than 4.0 Å [23,24]. The head-to-head aggregation subserves the exciton transfer between adjacent molecules to promote blue emission and prevents exciton quenching. In conclusion, $-OCF_3$ and $-SCF_3$ substituents decrease the packing.

The UV–vis absorption wavelengths of DATPC-OCF_3 (383 nm) and DATPC-SCF_3 (378 nm) in their solution states are about 22–27 nm blue shifted than that of DATPC (405 nm) shown in Fig. 4 (a). The fluorescence emission spectra show emission peaks at 440 nm (DATPC-OCF_3) and 435 nm (DATPC-SCF_3), which are 37–42 nm blue shifted than that of DATPC (477 nm). FWHM values of the fluorescence emission are 51 nm and 48 nm for DATPC-OCF_3 and DATPC-SCF_3, respectively, which are over 12 nm narrower as compared to that of DATPC (63 nm). Photoluminescence quantum yield (PLQY) in solution state of DATPC-OCF_3 and DATPC-SCF_3 are 50% and 42%, respectively, while that of DATPC is 47%, for details in Fig. S1 (ESI†). Fig. 4 (b) summarizes the UV–vis absorption and fluorescence emission spectra in solid state, with the same changing tendency as that of the solution state. The optical properties are listed in Table 2. The cyclic voltammetry (CV) are summarized in Fig. S2 (ESI†). In conclusion, $-OCF_3$ and $-SCF_3$

substituent modification can provide deep blue emission as well as higher color purity. The differential scanning calorimetry (DSC) in Fig. S3 (ESI†) and thermogravimetric analysis (TGA) in Fig. S4 (ESI†) were carried out to evaluate the thermal properties of our new materials and are summarized in Table 2. From the thermal property data, it is suggested that the additional $-OCF_3$ and $-SCF_3$ substituents can improve thermostability of the corresponding compounds, that may otherwise attribute to the unstable arylamine structure [25,26].

To study the effect of substituents on the hydrophobic property, contact angle measurements were also carried out and listed in Fig. 5. The contact angles of DATPC, DATPC-OCF_3 and DATPC-SCF_3 are 88.563°, 103.556° and 90.000°, respectively, obtained from an average value of five reasonable distribution points. Evidently, the hydrophobic property is enhanced by $-OCF_3$ and $-SCF_3$ substituents, providing better device stability.

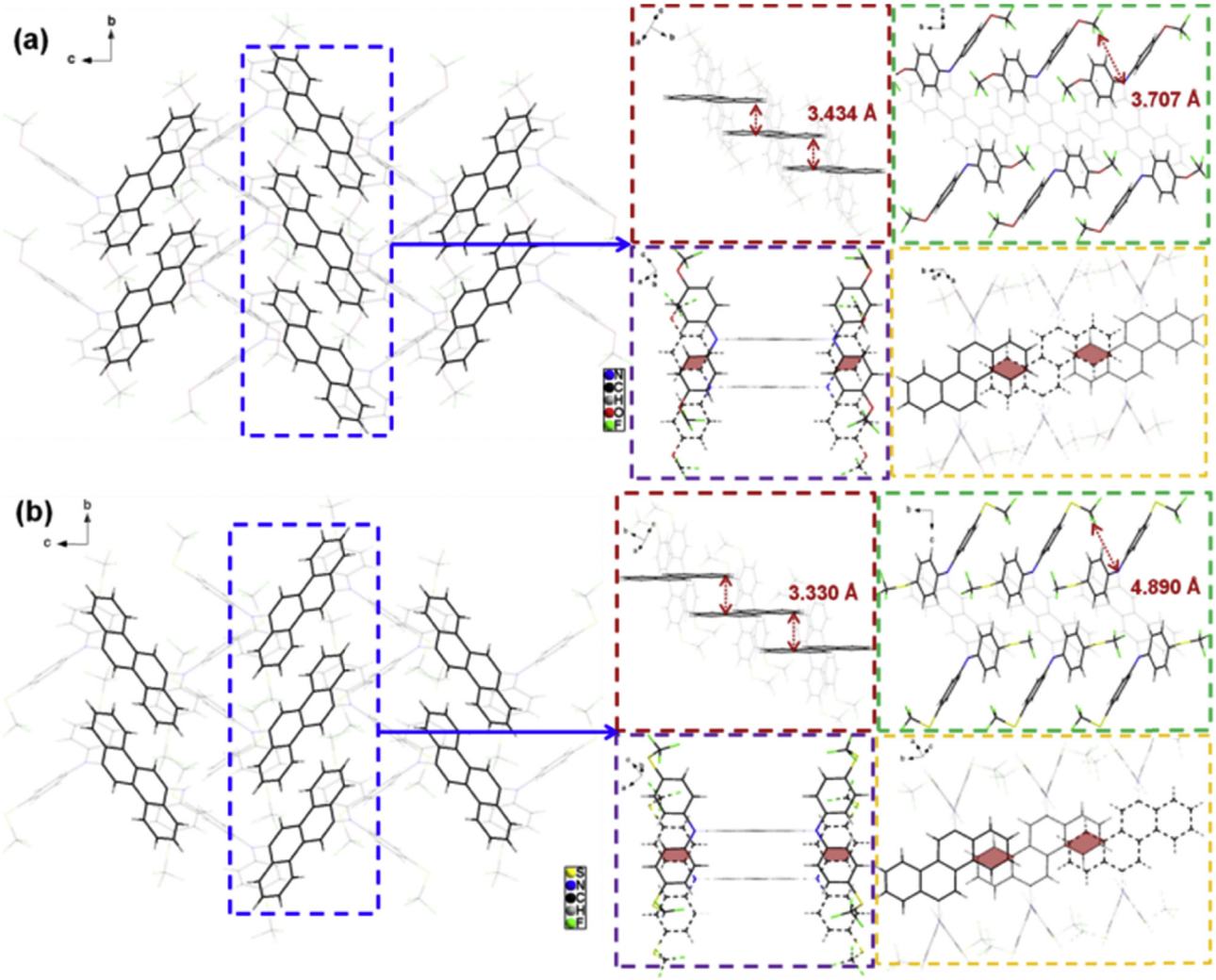

Fig. 3. Molecular packing structures of (a) DATPC-OCF_3 and (b) DATPC-SCF_3. Percentage and avoid co-planarity with chrysene, which results in the reduction of emission efficiency, causing bathochromic and broad emissions [8].

2.2. Electroluminescence properties

Although certain doped fluorescent OLEDs, which have been reported so far, can realize higher efficiency, undoped OLEDs are more attractive due to stable device performance and simple manufacturing processes [5]. Subsequently, blue undoped OLEDs with the structure [ITO/MoO_3 (1 nm)/TCTA (60 nm)/DATPC derivative (20 nm)/TPBi (40 nm)/LiF (1 nm)/Al (200 nm)] were fabricated. The optical and physical properties of the resulting devices are summarized in Fig. 6 and Table 3.

The EL spectra of DATPC derivative-based OLEDs are shown in Fig. 6 (a). The excimer emission peaks from new DATPC-OCF_3 (435 nm) and DATPC-SCF_3 (430 nm) are 25–30 nm shorter than that of DATPC (460 nm). FWHM value of DATPC-OCF_3 (49 nm) and DATPC-SCF_3 (50 nm) is 16 nm narrower than that of DATPC (66 nm). The EL spectra of DATPC-OCF_3 and DATPC-SCF_3 based OLED devices shows better blue color luminance and higher color purity. The EQE-current density curves of the devices are shown in Fig. 6 (b). The maximum EQE of DATPC-OCF_3 and DATPC-SCF_3 is obtained to be 2.70% and 3.05%, respectively, which is a significant improvement over that of DATPC (2.06%). Although EQE of DATPC-SCF_3 is highest, it gets roll-off quickly with the increase in current density. In general, the possible reason may be the difference in electron and hole mobility [27] as the material's energy barriers of hole-transporting and electron-transporting layer do not match very well. To further investigate this issue from the aspect of the concentration quenching effect, the time-resolved emission spectra were also recorded in Fig. S5 (ESI†) and Table S1 (ESI†). DATPC, DATPC-OCF_3 and DATPC-SCF_3 show exciton lifetimes of 3.7 ns, 3.4 ns and 2.0 ns, respectively, in solution state. The longer exciton lifetime can provide enough time for its transportation and aggregation in emitting layer, significantly for blue conventional fluorescence materials [28]. Fig. 6 (c) exhibits the CIE coordinate values for DATPC(0.17, 0.20), DATPC-OCF_3 (0.14, 0.09) and DATPC-SCF_3 (0.15, 0.06). It is noteworthy that we have unprecedentedly designed deep-blue emitters meeting the requirements of television displays with CIE coordinates of (0.14, 0.08) regulated by.

the National Television System Committee (NTSC); and High-Definition Television ITU-RBT.709 requiring CIE of (0.15, 0.06) for deep-blue emission [11]. Fig. 6 (d) shows OLED device structure incorporating DATPC, DATPC-OCF_3 or DATPC-SCF_3 as active emission layer. Tris(4-carbazoyl-9-ylphenyl)amine (TCTA) was applied as hole-transporting and exciton-blocking layer and 1,3,5-Tris(*N*-phenylbenzimidazol-2- yl)benzene (TPBi) was utilized as electron-transporting and exciton-blocking layer. In this article, we mainly focused on the innovation in material structure, and not too much

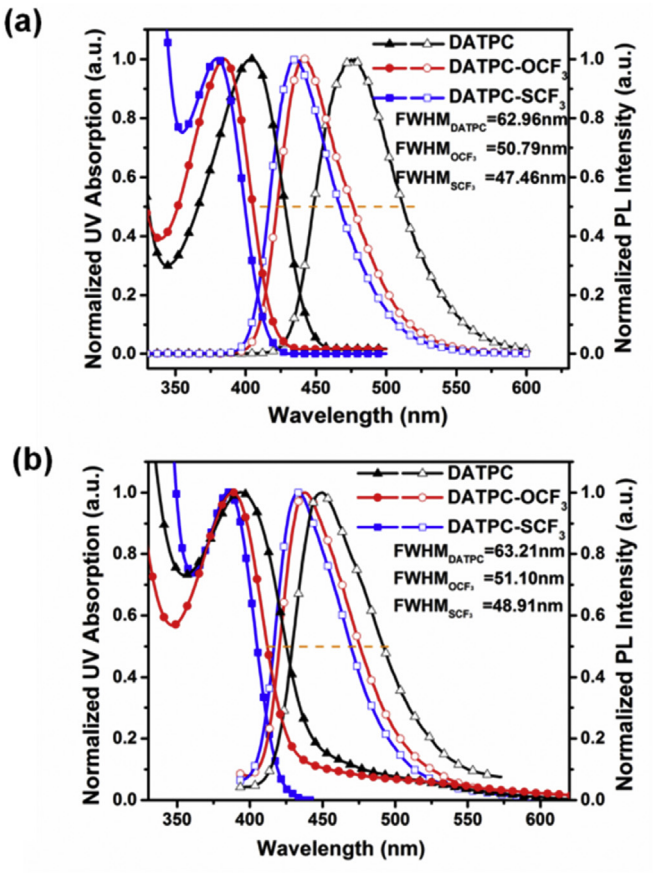

Fig. 4. The UV–vis absorption (solid dots) and fluorescence (hollow dots) spectra of DATPC, DATPC-OCF_3 and DATPC-SCF_3 (a) in anhydrous chloroform solution (1×10^{-5} M); (b) in the vacuum-deposited films (50 nm) on glass substrates.

on the exploration of device structure. But we believe that the roll-off problem of our new materials can be solved with a subsequent study to design appropriate device structure.

3. Experimental

3.1. Synthesis

DATPC, DATPC-OCF_3 and DATPC-SCF_3 were obtained from bromochrysene according to the reported procedure [8,29,30]. **Compound 8** (diphenylamine) was obtained from chemical company.

Compound 3 [bis(4-trifluoromethoxyphenyl)amine]: **Compound 1** (4-trifluoromethoxybromobenzene) (24.10 g, 0.1 mol) and **compound 2** (4-trifluoromethoxyphenylamine) (17.71 g, 0.1 mol) were added to dry toluene solution (300 mL). 1,1′-Bis(diphenylphosphino)ferrocene (**DPPF**) (6.65 g, 12 mmol), [1,1′-bis(diphenylphosphino)ferrocene]palladium(II) dichloride dichloromethane adduct [**(DPPF)PdCl$_2$.CH$_2$Cl$_2$**] (0.33 g, 0.4 mmol) and po + tassium tert-butoxide (**KOtBu**) (9.61 g, 0.1 mol) were added to the reaction mixture under nitrogen atmosphere. The reaction was stirred for 5 h at 120 °C. After completing the reaction, the mixture was poured into water (100 mL); the organic layer was extracted with ethyl acetate and distilled water. The obtained organic layer was isolated by silica gel column chromatography using the ethyl acetate: petroleum ether (1: 9) to get the oily product. Yield 67%. ^{1}H NMR (300 MHz, Chloroform-*d*) δ 7.15 (d, *J* = 8.4 Hz, 4H), 7.04 (d, *J* = 9.0 Hz, 4H), 5.72 (s, 1H). ^{13}C NMR (126 MHz, Chloroform-*d*) δ 143.65, 142.07, 122.79, 119.09.

Compound 6 [bis(4-trifluoromethylsufanylphenyl)amine]: **Compound 4** [4-(trifluoromethylsufanyl)bromobenzene] (21.42 g, 0.083 mol) and **compound 5** [4-(trifluoromethylsufanyl)phenylamine] (19.31 g, 0.1 mol) were added to dry toluene solution (300 mL). 1,1′-Bis(diphenylphosphino)ferrocene (**DPPF**) (6.65 g, 12 mmol), [1,1′-bis(diphenylphosphino)ferrocene]palladium(II) dichloride dichloromethane adduct [**(DPPF)PdCl$_2$.CH$_2$Cl$_2$**] (0.33 g, 0.4 mmol) and potassium tert-butoxide (**KOtBu**) (9.61 g, 0.1 mol) were added to the reaction mixture under nitrogen atmosphere. The reaction was stirred for 5 h at 120 °C. After completing the reaction, the mixture was poured into water (100 mL); the organic layer was extracted with ethyl acetate and distilled water. The obtained organic layer was isolated by silica gel column chromatography using the ethyl acetate: petroleum ether (1: 9) to get the oily product. Yield 73%. ^{1}H NMR (300 MHz, Chloroform-*d*) δ 7.57 (d, *J* = 8.6 Hz, 4H), 7.13 (d, *J* = 8.7 Hz, 4H), 6.08 (s, 1H). ^{13}C NMR

Table 2
Optical and thermal properties of DATPC, DATPC-OCF_3, and DATPC-SCF_3.

Compound	In Solution[a]			On Film[b]			PLQY[c](%)	T_g(C°)	T_m(C°)	T_d(C°)
	UV (nm)	PL (nm)	FWHM (nm)	UV (nm)	PL (nm)	FWHM (nm)				
DATPC	405	477	62.96	397	450	63.21	47	–	–	332
DATPC-OCF_3	383	440	50.79	385	438	51.10	50	95	237	335
DATPC-SCF_3	378	435	47.46	380	433	48.91	42	112	277	378

[a] 1×10^{-5}M in anhydrous chloroform.
[b] Film thickness is 50 nm on the glass.
[c] The solution-state in anhydrous chloroform relative quantum yield using the 2-Aminopyridine in 0.1 M H_2SO_4 as the reference.

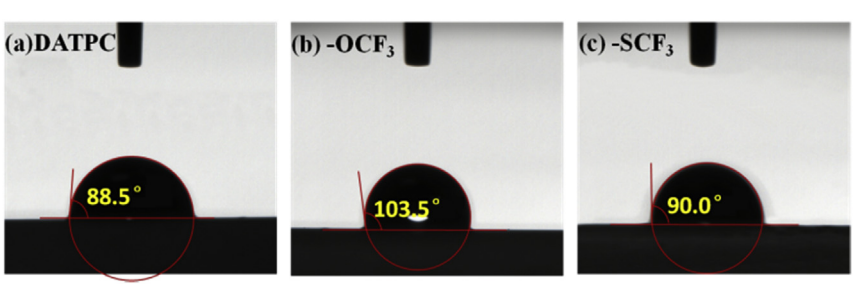

Fig. 5. Contact angles of (a) DATPC, (b) DATPC-OCF_3, and (c) DATPC-SCF_3 measured by 2 μL water spread over vacuum-deposited 50 nm films on the glass.

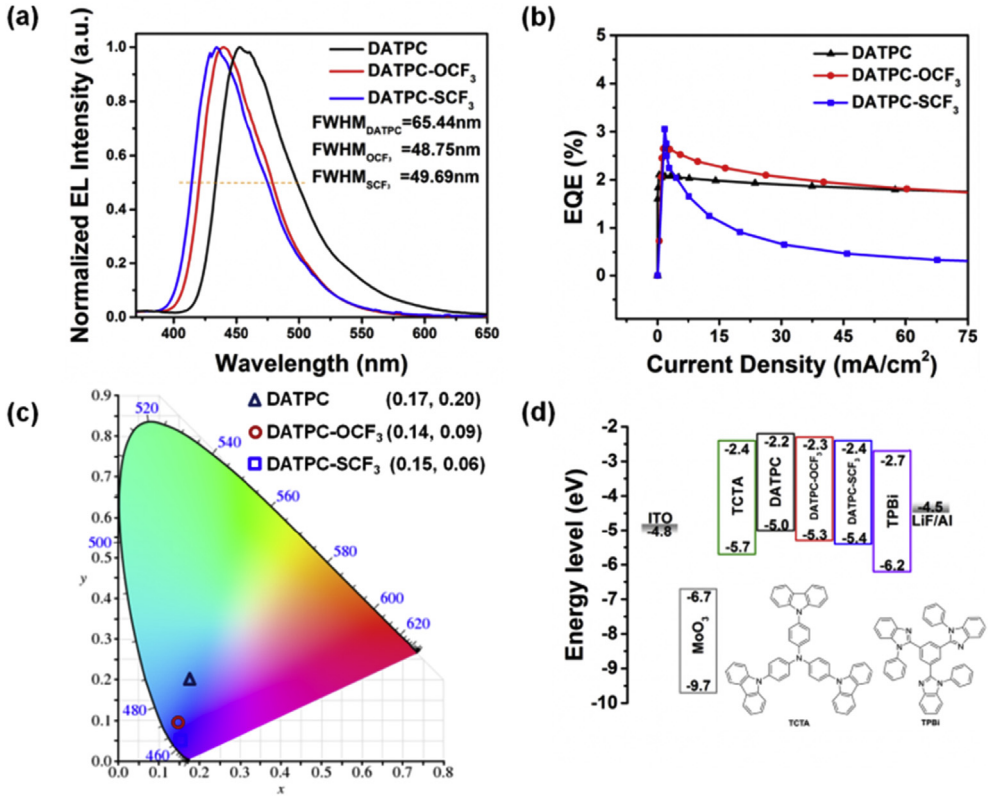

Fig. 6. (a) Normalized EL spectra of OLED devices made of DATPC, DATPC-OCF_3 and DATPC-SCF_3; (b) External quantum efficiency (EQE) versus current density; (c) CIE coordinate; (d) Device structure of DATPC and its derivatives as blue emitters.

Table 3
Electroluminescence efficiency of DATPC, DATPC-OCF_3 and DATPC-SCF_3 at 5 mA cm^{-2}

Compound	CIE (x,y)	EL_{max} (nm)	EL FWHM (nm)	V[a](V)	CE[b](cd A^{-1})	EQE_{max}
DATPC	(0.17, 0.20)	460	65.44	4.7	2.62	2.06
DATPC-OCF_3	(0.14, 0.09)	435	48.75	5.5	1.71	2.70
DATPC-SCF_3	(0.15, 0.06)	430	49.69	5.8	1.05	3.05

[a] Operating voltage.
[b] Current efficiency.

(126 MHz, Chloroform-*d*) δ 144.82, 138.53, 115.83, 60.84.

Compound 9 (DATPC): **Compound 7** (6,12-dibromochrysene) (1.94 g, 5 mmol) and **compound 8** (4.49 g, 20 mmol) were added to dry toluene solution (120 mL). Tris(dibenzylideneacetone)dipalladium(0) [**$Pd_2(dba)_3$**] (0.092 g, 0.1 mmol), tri-tert-butylphosphonium *tetra*fluoroborate [**$P(tBu)_3HBF_4$**] (0.029 g, 0.2 mmol) and potassium tert-butoxide (**KOtBu**) (1.68 g, 1.5 mmol) were added to the reaction mixture under nitrogen atmosphere. The reaction was stirred for 5 h at 110 °C. After completing the reaction, the mixture was poured into water (50 mL); the organic layer was extracted with dichloromethane and distilled water. The obtained organic layer was isolated by silica gel column chromatography using the dichloromethane: petroleum ether (1:3). Yield 19%. ^{1}H NMR (300 MHz, Chloroform-*d*) δ = 8.55 (d, *J* = 8.8 Hz, 4H), 8.11 (d, *J* = 8.3 Hz, 2H), 7.59 (t, *J* = 7.6 Hz, 2H), 7.47 (t, *J* = 7.5 Hz, 2H), 7.21 (d, *J* = 7.6 Hz, 8H), 7.15 (d, *J* = 8.0 Hz, 8H), 6.96 (t, *J* = 7.2 Hz, 4H). ^{13}C NMR (126 MHz, Chloroform-*d*) δ 129.21, 129.18, 129.10, 126.96, 126.90, 126.85, 125.07, 124.99, 123.62, 121.95, 121.86, 121.77. HRMS(APCI): *m*/*z* calcd for $C_{42}H_{31}N_2$ $[M+H]^+$ 563.2482; found 563.2476.

Compound 10 (DATPC-OCF_3): **Compound 7** (5.32 g, 13.71 mmol) and **compound 3** (10.17 g, 30.20 mmol) were added to dry toluene solution (150 mL). Tris(dibenzylideneacetone)dipalladium(0) [**$Pd_2(dba)_3$**] (0.25 g, 0.27 mmol), tri-tert-butylphosphonium *tetra*fluoroborate [**$P(tBu)_3HBF_4$**] (0.16 g, 0.55 mmol) and potassium tert-butoxide (**KOtBu**) (3.78 g, 39.30 mmol) were added to the reaction mixture under nitrogen atmosphere. The reaction was stirred for 5 h at 110 °C. After completing the reaction, the mixture was poured into water (50 mL); the organic layer was extracted with dichloromethane and distilled water. The obtained organic layer was isolated by silica gel column chromatography using the dichloromethane: petroleum ether (1: 3). Yield 63%. ^{1}H NMR (300 MHz, Chloroform-*d*) δ = 8.62–8.53 (m, 4H), 8.04 (dd, *J* = 8.3, 1.3 Hz, 2H), 7.67 (ddd, *J* = 8.4, 6.9, 1.4 Hz, 2H), 7.54 (ddd, *J* = 8.1, 6.9, 1.1 Hz, 2H), 7.17–7.05 (m, 16H). ^{13}C NMR (75 MHz, Chloroform-*d*) δ = 146.63, 143.99, 142.22, 132.06, 130.17, 128.14, 127.67, 127.62, 124.75, 123.91, 122.74, 122.64, 122.40, 118.97. HRMS(APCI): *m*/*z* calcd for $C_{46}H_{27}F_{12}O_4N_2$ $[M+H]^+$899.1774; found 899.0159.

Compound 11 (DATPC-SCF_3): **Compound 7** (4.10 g, 10.55 mmol) and **compound 6** (8.57 g, 23.22 mmol) were added to dry toluene solution (120 mL). Tris(dibenzylideneacetone)dipalladium(0) [**$Pd_2(dba)_3$**] (0.19 g, 0.21 mmol), tri-tert-butylphosphonium *tetra*fluoroborate [**$P(tBu)_3HBF_4$**] (0.12 g, 0.42 mmol) and potassium tert-

butoxide (**KOtBu**) (3.04 g, 31.65 mmol) were added to the reaction mixture under nitrogen atmosphere. The reaction was stirred for 5 h at 110 °C. After completing the reaction, the mixture was poured into water (50 mL); the organic layer was extracted with dichloromethane and distilled water. The obtained organic layer was isolated by silica gel column chromatography using the dichloromethane: petroleum ether (1: 3). Yield 71%. ^{1}H NMR (300 MHz, Chloroform-*d*) δ = 8.68–8.58 (m, 4H), 7.98 (dd, *J* = 8.3, 1.3 Hz, 2H), 7.69 (ddd, *J* = 8.4, 6.9, 1.4 Hz, 2H), 7.60–7.55 (m, 2H), 7.55–7.47 (m, 8H), 7.24–7.14 (m, 8H). ^{13}C NMR (75 MHz, Chloroform-*d*) δ = 149.31, 141.29, 137.84, 131.93, 128.29, 127.82, 127.73, 124.29, 123.83, 123.11, 121.94, 116.68. HRMS(APCI):*m*/*z* calcd for C46H27F12N2S4 $[M+H]^+$ 963.0860; found: 963.8682.

3.2. General information

The ^{1}H-NMR and ^{13}C-NMR spectra were recorded on Bruker Avance 300 spectrometers. The high-resolution mass spectra (HRMS) were recorded on TOFMS(APCI), 4800 PLUS, ABI.

The theoretical calculation of the HOMO and LUMO energy levels and dimer structure were done by Spartan software at DFT B3LYP/6-31G* levels of theory. The Experimental data of HOMO and LUMO energy levels were calculated from redox potential in CV curve.

The UV–vis spectra were obtained by using a PerkinElmer Lambda 1050 UV/Vis/NIR spectrometer. The photoluminescence spectra were obtained by a PerkinElmer luminescence spectrometer.

3.3. Single crystal X-ray diffraction

CCDC 1522077 and 1503591 contain the supplementary crystallographic data for DATPC-OCF_3 or DATPC-SCF_3 respectively. These data are provided free of charge by The Cambridge Crystallographic Data Centre.

4. Conclusions

This article investigates the effect of super hydrophobic and strong electron withdrawing groups $-OCF_3$ and $-SCF_3$ to realize highly efficient deep blue fluorescence with more pure color quality, higher thermostability and better moisture resistant properties. The photophysical and optoelectronic properties have been interpreted with the help of theoretical calculations based on the DFT approach along with molecular packing study of their single crystal X-ray analysis. Single layer undoped devices achieved the maximum EQE 3.05% and CIE coordinate values of (0.14, 0.09) and (0.15, 0.06) for DATPC-OCF and DATPC-SCF_3, respectively, exactly meeting High-Definition Television ITU-R BT.709 requirement of CIE coordinates of (0.15, 0.06) for deep-blue emission. We believe the theory prior to experiment, accurately predicting the material's properties, can promote the experience in molecular formulation and designing.

Acknowledgements

This work was financially supported by the Shenzhen Peacock Program (KQTD2014062714543296), Guangdong Key Research Project (2014B090914003, 2015B090914002), Shenzhen Key Laboratory of Organic Optoelectromagnetic Functional Materials of Shenzhen Science and Technology Plan (ZDSYS20140509094114164), Natural Science Foundation of Guangdong Province (2014A030313800), Shenzhen Science and Technology Research Grant (JCYJ20140509093817690, JCYJ20150629144328079, JCYJ20160331095335232), Nanshan Innovation Agency Grant (KC2015ZDYF0016A), National Basic Research Program of China (973 Program, 2015CB856505), Guangdong Academician Workstation (2013B090400016).

Appendix A. Supplementary data

Supplementary data related to this article can be found at http://dx.doi.org/10.1016/j.dyepig.2016.12.034.

References

[1] Tang CW, VanSlyke SA. Organic electroluminescent diodes. Appl Phys Lett 1987;51(12):913.
[2] Middleton AJ, Marshall WJ, Radu NS. Elucidation of the structure of a highly efficient blue electroluminescent material. J Am Chem Soc 2003;125(4):880–1.
[3] Jeon SO, Yook KS, Joo CW, Lee JY. Phenylcarbazole-based phosphine oxide host materials for high efficiency in deep blue phosphorescent organic light-emitting diodes. Adv Funct Mater 2009;19(22):3644–9.
[4] Xing X, Xiao L, Zheng L, Hu S, Chen Z, Qu B, et al. Spirobifluorene derivative: a pure blue emitter (CIEy ≈ 0.08) with high efficiency and thermal stability. J Mater Chem 2012;22(30):15136.
[5] Zhang Q, Tsang D, Kuwabara H, Hatae Y, Li B, Takahashi T, et al. Nearly 100% internal quantum efficiency in undoped electroluminescent devices employing pure organic emitters. Adv Mater 2015;27(12):2096–100.
[6] Zhang Y, Lai S-L, Tong Q-X, Lo M-F, Ng T-W, Chan M-Y, et al. High efficiency nondoped deep-blue organic light emitting devices based on imidazole-π-triphenylamine derivatives. Chem Mater 2012;24(1):61–70.
[7] Li J, Zhang Q. Linearly fused azaacenes: novel approaches and new applications beyond field-effect transistors (FETs). ACS Appl Mater Interfaces 2015;7(51):28049–62.
[8] Shin H, Jung H, Kim B, Lee J, Moon J, Kim J, et al. Highly efficient emitters of ultra-deep-blue light made from chrysene chromophores. J Mater Chem C 2016;4(17):3833–42.
[9] Nishimura KF, Kenichi; Iwakuma, Toshihiro; Hosokawa, Chishio.. WO 2009008348. In: Kosan I, editor. Espacenet. Japan2009.
[10] Zhang Q, Li J, Shizu K, Huang S, Hirata S, Miyazaki H, et al. Design of efficient thermally activated delayed fluorescence materials for pure blue organic light emitting diodes. J Am Chem Soc 2012;134(36):14706–9.
[11] Hu J-Y, Pu Y-J, Satoh F, Kawata S, Katagiri H, Sasabe H, et al. Bisanthracene-based donor-acceptor-type light-emitting dopants: highly efficient deep-blue emission in organic light-emitting devices. Adv Funct Mater 2014;24(14):2064–71.
[12] Aziz H, Popovic ZD, Hu N-X, Hor A-M, Xu G. Degradation mechanism of small molecule-based organic light-emitting devices. Science 1999;283(5409):1900–2.
[13] So F, Kondakov D. OLEDs: degradation mechanisms in small-molecule and polymer organic light-emitting diodes (adv. Mater. 34/2010). Adv Mater 2010;22(34):3762–77.
[14] Zheng H, Huang Y, Weng Z. Recent advances in trifluoromethylthiolation using nucleophilic trifluoromethylthiolating reagents. Tetrahedron Lett 2016;57(13):1397–409.
[15] Valeur B. Molecular fluorescence: principles and applications. 2002.
[16] Lee CW, Lee JY. Low driving voltage and high power efficiency in blue phosphorescent organic light-emitting diodes using aromatic amine derivatives with diphenylsilyl linkage. Synth Met 2013;167:1–4.
[17] Li G, Zhao Y, Li J, Cao J, Zhu J, Sun XW, et al. Synthesis, characterization, physical properties, and OLED application of single BN-fused perylene diimide. J Org Chem 2015;80(1):196–203.
[18] Hansch C, Leo A, Taft RW. A survey of Hammett substituent constants and resonance and field parameters. Chem Rev 1991;91(2):165–95.
[19] Li J, Yan F, Gao J, Li P, Xiong W-W, Zhao Y, et al. Synthesis, physical properties and OLED performance of azatetracenes. Dyes Pigments 2015;112:93–8.
[20] Li G, Xiong W-W, Gu P-Y, Cao J, Zhu J, Ganguly R, et al. 1,5,9-Triaza-2,6,10-triphenylboracoronene: BN-Embedded analogue of coronene. Org Lett 2015;17(3):560–3.
[21] Kawabata K, Saito M, Osaka I, Takimiya K. Very small bandgap π-conjugated polymers with extended thienoquinoids. J Am Chem Soc 2016;138(24):7725–32.
[22] Ooyama Y, Yamada T, Fujita T, Harima Y, Ohshita J. Development of D-[small pi]-Cat fluorescent dyes with a catechol group for dye-sensitized solar cells based on dye-to-TiO2 charge transfer. J Mater Chem A 2014;2(22):8500–11.
[23] Dong Y, Xu B, Zhang J, Tan X, Wang L, Chen J, et al. Piezochromic luminescence based on the molecular aggregation of 9,10-Bis((E)-2-(pyrid-2-yl)vinyl) anthracene. Angew Chem 2012;51(43):10782–5.
[24] Meyer EA, Castellano RK, Diederich F. Interactions with aromatic rings in chemical and biological recognition. Angew Chem 2003;42(11):1210–50.
[25] Gronnier C, Bel PFd, Henrion G, Kramer S, Gagosz F. Divergent product selectivity in gold- versus silver-catalyzed reaction of 2-Propynyloxy-6-fluoropyridines with arylamines. Org Lett 2014;16(8):2092–5.
[26] Gornostaev LM, Dolgushina LV, Titova NG, Arnol'd EV, Lavrikova TI. Synthesis

of 3-alkyl-5-arylamino-6,11-dihydro-3 H-anthra[1,2- d]-[1,2,3]triazole-6,11-dione 2-oxides by nitrosation of 3-alkylamino-5-arylamino-6 H-anthra[1,9-cd]isoxazol-6-ones. Russ J Org Chem 2006;42(9):1364–7.

[27] Kim J-S, Friend RH, Grizzi I, Burroughes JH. Spin-cast thin semiconducting polymer interlayer for improving device efficiency of polymer light-emitting diodes. Appl Phys Lett 2005;87(2):023506.

[28] Savvate'ev V, Friedl JH, Zou L, Shinar J, Christensen K, Oldham W, et al. Nanosecond transients in the electroluminescence from multilayer blue organic light-emitting devices based on 4,4[sup ′]-bis(2,2[sup ′]diphenyl vinyl)-1,1[sup ′]-biphenyl. Appl Phys Lett 2000;76(12):1501.

[29] V. Rostovtsev LB, H. Meng, A. Merlo, N. Herron, J. Chesterfield. WO2008147721A1. US2008.

[30] Li J, Zhang Q. Mono- and oligocyclic aromatic ynes and diynes as building blocks to approach larger acenes, heteroacenes, and twistacenes. Synlett 2013;24:686–96.